

Infrared investigation of the phonon spectrum in the frustrated spin cluster compound
 $\text{FeTe}_2\text{O}_5\text{Cl}$

This article has been downloaded from IOPscience. Please scroll down to see the full text article.

2009 J. Phys.: Condens. Matter 21 375401

(<http://iopscience.iop.org/0953-8984/21/37/375401>)

View [the table of contents for this issue](#), or go to the [journal homepage](#) for more

Download details:

IP Address: 129.252.86.83

The article was downloaded on 30/05/2010 at 05:01

Please note that [terms and conditions apply](#).

Infrared investigation of the phonon spectrum in the frustrated spin cluster compound $\text{FeTe}_2\text{O}_5\text{Cl}$

F Pfuner¹, L Degiorgi¹, H Berger² and L Forró²

¹ Laboratorium für Festkörperphysik, ETH Zürich, CH-8093 Zürich, Switzerland

² Institut de Physique de la Matière Complexe (IPMC), EPF Lausanne, CH-1015 Lausanne, Switzerland

Received 30 June 2009, in final form 4 August 2009

Published 21 August 2009

Online at stacks.iop.org/JPhysCM/21/375401

Abstract

We present our optical investigations on the frustrated spin cluster compound $\text{FeTe}_2\text{O}_5\text{Cl}$, which develops a long-range antiferromagnetic order below 10 K. We measure the optical reflectivity from the far-infrared to the ultraviolet with polarized light. We focus our attention on the lattice dynamics by discussing the infrared-active modes. Our findings reveal a polarization dependence of the vibrational modes but which do not seem to be affected by structural anomalies linked to the magnetically ordered state at low temperatures.

(Some figures in this article are in colour only in the electronic version)

The effects of quantum fluctuations have been at the center of interest in the past few years from both the theoretical and experimental points of view. Quantum fluctuations notoriously suppress long-range magnetically ordered ferro- or antiferromagnetic phases, are mainly effective in low-dimensional quantum spin systems and originate from the interplay between reduced dimensionality, small spin and magnetic frustration [1]. The interest in such phenomena has principally been motivated by peculiarities in the physical properties of the two-dimensional superconducting cuprates as well as of related transition metal oxides. Very often the two-dimensional exchange topologies provide the basis for an effective interplay between competing interactions with remaining spin anisotropies, thus leading to magnetic frustration. Spins in a frustrated magnet cannot simultaneously minimize the energies of their local interactions. A strongly frustrated system is said to have a high density of low-energy excitations or soft modes that correspond to fluctuations between these energetically equivalent configurations. A large wealth of spectroscopic tools may be suitable in order to chase those magnetically driven excitations [1].

Several materials have been designed so far as prototype examples of low-dimensional quantum spin systems [1]. There has been much experimental activity directed at spin $S = 1/2$ materials involving Cu^{2+} ions with a $3d^9$ configuration, or Ti^{3+} and V^{4+} systems in the d^1 configuration, among which we mention the spin-Peierls CuGeO_3 systems, the

charge-ordered NaV_2O_5 compound with broken translational symmetry, the TiOX ($X = \text{Cl}$ and Br) compounds or the $\text{Cu}_2\text{Te}_2\text{O}_5\text{X}_2$ ($X = \text{Cl}$, Br) materials with their unconventional magnetic ordering [1–3]. Furthermore, the $\text{Ni}_5\text{Te}_4\text{O}_{12}\text{X}_2$ ($X = \text{Cl}$ and Br) compounds in the $3d^8$ electron configuration with $S = 1$ and negligible or quenched orbital momentum raised some interest as well [1, 4].

During the past few years novel synthesis concepts have been developed in order to systematically design new low-dimensional spin-frustrated inorganic compounds that comprise Fe^{3+} ions. One of these synthesis concepts is based on forming oxohalides involving p-element cations that are in the oxidation state where they have a stereochemically active lone pair (e.g. Te^{4+}). The presence of a stereochemically active lone pair allows for asymmetric or one-sided coordination around the lone pair cation. The search for new low-dimensional configurations in the $\text{Fe}^{3+}\text{--Te}^{4+}\text{--O--X}$ ($X = \text{Cl}$ and Br) systems led to the layered transition metal oxohalide $\text{FeTe}_2\text{O}_5\text{X}$ ($X = \text{Cl}$ and Br). Figure 1 displays the crystal structure from the perspective of the (ab) and (bc) planes [5]. The title compound crystallizes in the monoclinic space group $P2_1/c$, with layers (i.e. (bc) plane) built of edge-sharing FeO_6 octahedra forming $(\text{Fe}_4\text{O}_{16})^{20-}$ units which are linked by the $(\text{Te}_4\text{O}_{10}\text{X}_2)^{6-}$ groups and are stacked along the a axis [5]. The layers have no net charge and are only weakly connected via van der Waals forces to adjacent layers. There are four crystallographically different Te^{4+} cations, which

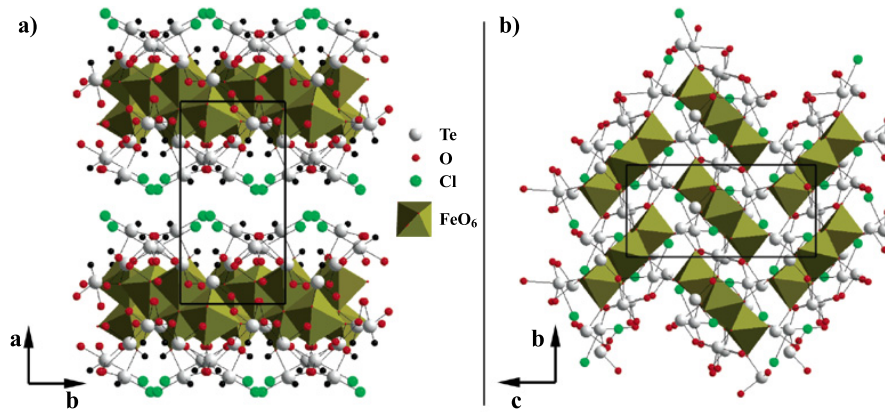


Figure 1. Crystal structure of $\text{FeTe}_2\text{O}_5\text{X}$, showing (a) the (ab) -plane perspective (i.e. view along the c axis) with the layers of the edge-sharing FeO_6 octahedra and (b) the (bc) -plane perspective (i.e. view along the a axis). The black spheres represent the stereochemically active lone pair [5].

all can be described as having an asymmetric one-sided coordination with different numbers of ligands. Each layer can be considered as an infinite two-dimensional molecule, where the halide anions and the stereochemically active lone pairs of the Te^{4+} cations protrude from the layers. From the crystal chemistry point of view, one can then state that the title compound is unique in two ways: it is the first one belonging to the class of $\text{Fe}^{3+}\text{-Te}^{4+}\text{-O-X}$ ($\text{X} = \text{Cl}$ and Br) systems and it also possesses a unique FeTe_2OX tetrahedron around Te^{4+} , where furthermore Te^{4+} has the classical one-sided three-coordination with both oxygen and a halide instead of only one of the two ligands.

Magnetic susceptibility measurements show a Curie–Weiss behavior for temperatures above about 100 K and a broad maximum at $T_{\text{max}} = 41.8$ K, typical for a four-spin cluster of coupled $\text{Fe}(111)$ ions in the high-spin state. Field-cooled and zero-field-cooled measurements show no traceable hysteresis. The effective magnetic moments, obtained from the fits of the reciprocal susceptibilities with a modified Curie–Weiss law, are very close to $5.92 \mu_{\text{B}}$ as expected for Fe^{3+} with a d^5 electronic configuration and a high-spin 6S ($S = 5/2$, $g = 2$) ground state [5]. The negative paramagnetic Curie temperature $\Theta_{\text{CW}} \sim -124$ K indicates predominant antiferromagnetic exchange interactions. At $T_N \sim 10$ K the susceptibility of $\text{FeTe}_2\text{O}_5\text{Cl}$ is characterized by a kink, apparently due to the onset of long-range antiferromagnetic ordering. Obviously, magnetic frustration and the reduced inter-cluster exchange are the reason for the small long-range ordering temperature T_N (i.e. the frustration parameter $f = |\Theta_{\text{CW}}/T_N| \sim 10$) [5]. A theoretical modeling of the susceptibility led to a scenario where frustration derives from intra-tetramer antiferromagnetic exchange interaction. Evidence for magnetic instabilities has also been confirmed with specific heat experiments [5].

In this brief report, we present and discuss our optical data collected on a high quality $\text{FeTe}_2\text{O}_5\text{Cl}$ single crystal. The aim of our work was to spectroscopically characterize the title compound with respect to its magnetic phase and specifically address its phonon spectrum, which sheds light on the lattice dynamics. It is well established, that magnetic excitations,

while in principle not infrared-active, can, under favorable conditions, carry a finite electric dipole moment [6–9].

Single crystals of $\text{FeTe}_2\text{O}_5\text{Cl}$ were grown by the standard chemical vapor phase method. Mixtures of commercial ‘Pro-analyze’ Fe_2O_3 , TeO_2 and FeCl_3 powder in molar ratio 1:6:1 were heated at 500°C for 50 h in evacuated sealed quartz tubes. Approximately 10 g of reactants were pulverized and sealed in the quartz tubes with Cl_2 (800 mbar at room temperature) as the transport gas for the crystal growth. The ampules were then placed in two zone gradient furnaces. The optimum temperatures at the source and deposition zones for the growth of single crystals were 500°C and 400°C , respectively. Each experimental run lasted for 250–350 h. In the center of the ampule, large yellow $\text{FeTe}_2\text{O}_5\text{Cl}$ platelets formed with a maximum size of $12 \times 10 \times 0.2 \text{ mm}^3$. X-ray diffraction data confirmed the single phase of the obtained crystals.

The shiny and large optical surface of our specimens allows high quality optical investigations. We collected optical reflectivity ($R(\omega)$) data over a wide frequency spectral range extending from the far-infrared (FIR) up to the ultraviolet (UV), i.e. 5 meV–7 eV, with light polarized along two orthogonal directions within the (bc) plane. The polarization directions were chosen in such a way that the $R(\omega)$ signal displays the largest anisotropy among them. In the infrared spectral range we made use of a Fourier interferometer equipped with a magneto-optical cryostat, allowing the temperature to be varied from 2 to 300 K and the magnetic field from 0 up to 7 T. Details pertaining to the experiment can be found elsewhere [10, 11].

Figure 2(a) presents the FIR optical reflectivity at 300 K for both light polarizations, while the inset of figure 4 illustrates the features in $R(\omega)$ up to the UV spectral range. The spectra are characterized by a number of sharp lines, which appear at different frequencies along the two polarization directions. Figure 2(b) displays $R(\omega)$ at two selected temperatures at zero and 6 T for one of the two polarization directions³. By lowering the temperature we observe the expected sharpening of the modes, particularly in the FIR

³ Along the other polarization direction (not shown) we obtained a similar trend as far as the temperature and magnetic field dependence is concerned.

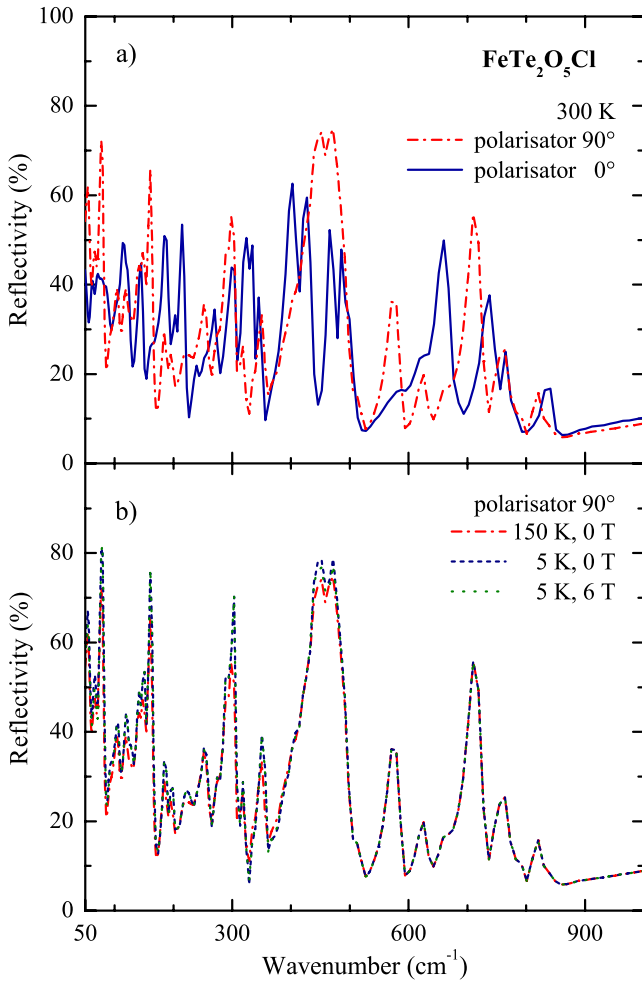


Figure 2. (a) Reflectivity $R(\omega)$ of $\text{FeTe}_2\text{O}_5\text{Cl}$ measured at 300 K in the FIR energy range for light polarized along two orthogonal directions within the (bc) plane. (b) $R(\omega)$ at selected temperatures and magnetic fields for one of the two investigated polarization directions (see footnote 3).

energy interval. Nevertheless, we did not find any changes in the spectra, such as the appearance of additional modes with decreasing temperature. We also did not observe any magnetic field dependence at all investigated temperatures, so we will focus our attention on the polarization dependence of the spectra.

We can then exploit the Kramers–Kronig (KK) procedure applied on $R(\omega)$, collected here over several decades in energy (inset figure 4), in order to extract all optical functions [10, 11]. To this purpose, we first extrapolate $R(\omega)$ below 5 meV with a constant term, because of the insulating nature of our compound, while we extend $R(\omega)$ at high frequencies with $R(\omega) \sim \omega^{-2}$ up to ~ 20 eV and thereafter with $R(\omega) \sim \omega^{-4}$ to simulate the excitation into the continuum [10, 11]. Figure 3 then displays the real part $\sigma_1(\omega)$ of the optical conductivity in the FIR spectral range. The insulating nature of $\text{FeTe}_2\text{O}_5\text{Cl}$ is again underlined by the vanishingly small static limit of $\sigma_1(\omega \rightarrow 0)$.

Before addressing the phonon spectrum we first give a look to $\sigma_1(\omega)$ at high frequencies. Figure 4 emphasizes

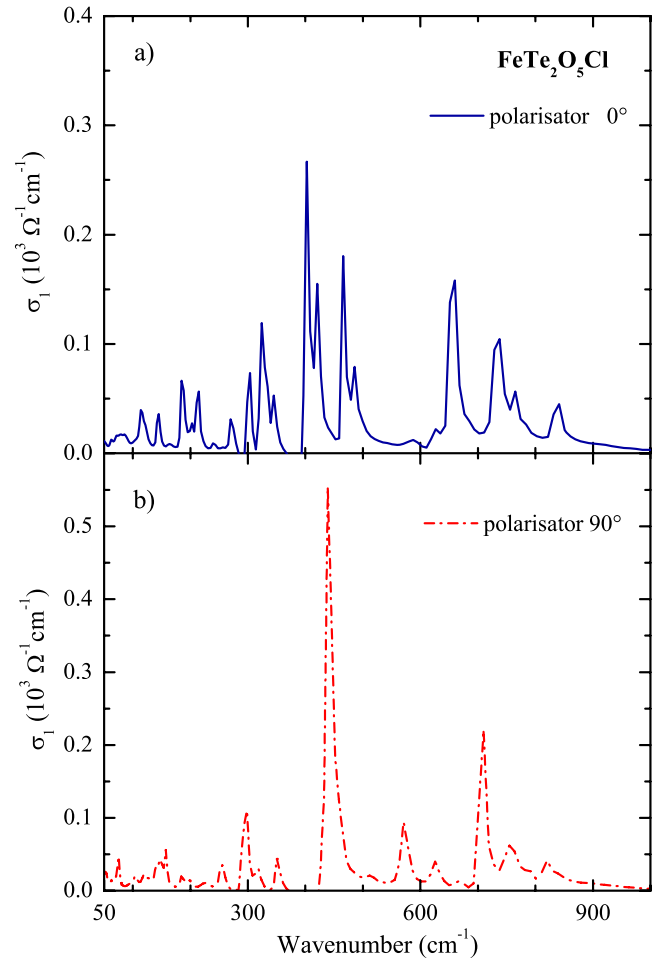


Figure 3. Real part $\sigma_1(\omega)$ of the optical conductivity at 300 K in the FIR energy range for light polarized along two orthogonal directions within the (bc) plane (figure 2(a)). The sharp phonon modes are well evident.

indeed the visible–ultraviolet spectral range of $\sigma_1(\omega)$, which is dominated by the broad feature approximately centered at $2.5 \times 10^4 \text{ cm}^{-1}$. Overlapped with its low frequency tail, two absorptions can be recognized: the shoulder at 10^4 cm^{-1} and the peak at $1.8 \times 10^4 \text{ cm}^{-1}$. These excitations are in principle ascribed to the electronic interband transitions, mainly involving the Fe 3d and the Te 4d and 5p states. A precise assignment of these excitations awaits nonetheless a thorough band-structure and joined-density-of-states calculation, respectively.

The major focus here is on the lattice dynamics for which the analysis of the phonon spectrum is of relevance. All sharp peaks, seen in the spectra for both polarization directions below 1000 cm^{-1} , originate from lattice vibrational modes. The number of phonon modes expected in $\text{FeTe}_2\text{O}_5\text{Cl}$ can be estimated by the space group analysis. The unit cell of the monoclinic title compound encountered 18 atoms, all having a Wyckoff position **e** corresponding to a multiplicity of 4. This leads to 72 effective atom positions and to a total of 216 expected modes (i.e. 72×3 , where 3 is the number of space directions). Using the SMODES code [12] we achieve the

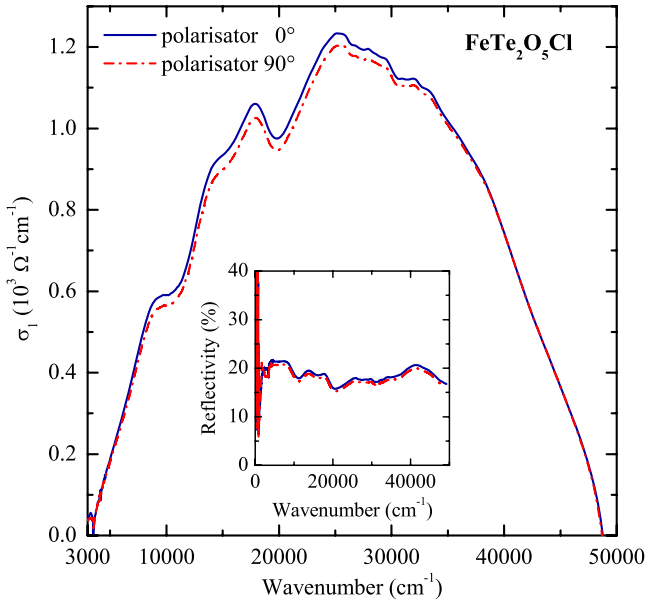


Figure 4. Real part $\sigma_1(\omega)$ of the optical conductivity of $\text{FeTe}_2\text{O}_5\text{Cl}$ measured at 300 K for light polarized along two orthogonal directions within the (bc) plane from the mid-infrared to the ultraviolet energies. The features due to electronic interband transitions are here emphasized. The inset displays the overall $R(\omega)$ for both polarizations, highlighting the ultraviolet spectral range (for details of $R(\omega)$ in FIR, see figure 2(a)).

following distribution of modes:

$$\Gamma^{\text{optical}} = 54A_g^{(R)} + 54B_g^{(R)} + 53A_u^{(\text{IR})} + 52B_u^{(\text{IR})},$$

and

$$\Gamma^{\text{acoustic}} = 1A_u + 2B_u,$$

where (R) stands for Raman-active and (IR) for infrared-active. Therefore, a total of 105 modes should be IR-active. Because of the monoclinic structure, projections of the a axis along c leads in principle to a situation where relatively weak modes might contaminate the phonon spectrum within the (bc) plane. If we assume as a first approximation that the modes along the a axis are nevertheless weak enough to be relevant, we can then predict a total of ~ 72 phonons within the (bc) plane. This estimation only takes into account the displacements of the 18 atoms in the unit cell along the b and c directions for both irreducible representations A_u (2×18) and B_u (2×18). For both A_u and B_u symmetries, the relative atomic displacements occur, however, in the same direction. This means that it is fairly impossible to single them out with respect to their symmetry in our polarized spectra. Another issue, hindering a precise phonon assignment, concerns the building blocks of the layer, which are indeed similar but oriented differently (i.e. the same arrangement of atoms; however, rotated or tilted with respect to each other). This results in a herringbone-like pattern configuration (figure 1(b)). As a consequence of that several phonon modes belong to different symmetries but may occur at an equivalent energy scale. Such modes will overlap and will not be resolved separately. These latter arguments clearly suggest that in the

measured spectra we cannot expect to detect all 72 modes foreseen for the (bc) -plane experimental configuration. The total number of observable modes will be reduced by roughly a factor of two. In our spectra (figure 3) we count a total of about 38 modes for both polarizations, which is pretty close to the expectation. The low-energy modes (i.e. $\omega \lesssim 300 \text{ cm}^{-1}$) are ascribed to the vibrational states between the FeO_6 blocks while those at high energies are more probably due to intra-block vibrational modes.

In presenting the data we have already pointed out the very weak temperature dependence of the phonon spectrum, where the sharp lines in $\sigma_1(\omega)$ just get narrow with decreasing temperature. We did not observe any remarkable anomalies on the increase of the mode strength, the appearance of new modes or the splitting of existing phonons below $T_N \sim 10 \text{ K}$ [5]. These latter effects would be considered as a consequence of lattice distortion, occurring with the magnetic transition and the related symmetry breaking. Our results on $\text{FeTe}_2\text{O}_5\text{Cl}$ are similar to what are encountered in $\text{Ni}_5\text{Te}_4\text{O}_{12}\text{X}_2$ [4] as well as in $\text{Cu}_2\text{Te}_2\text{O}_5\text{X}_2$ [2] but are quite different from the results in the spin-web Cu_3TeO_6 [13], where a new mode was indeed found to develop at temperatures lower than the Néel temperature. The present findings also do not give evidence for a Fano-like shape in the infrared-active phonons, as was seen in TiOCl , which would suggest an interaction between the lattice vibrations and a continuum of low frequency (spin) excitations [3]. In contrast to TiOCl , we did not establish any redistribution of spectral weight as a function of temperature either, which could lead to the identification of the pseudo-spin gap [3].

In summary, we have provided an FIR investigation of the phonon spectrum of $\text{FeTe}_2\text{O}_5\text{Cl}$ and identified some of the expected lattice vibrational modes. The absence of any link between the transition at T_N and the electrodynamic response seems to exclude a tight connection between the lattice dynamics, the electronic spectrum and the magnetic transition, and therefore seems to indicate that mechanisms such as charge bi-magnons or phonon-assisted multi-magnon optical absorption may be inappropriate for the title compound [1]. More light into the magnetic excitations and into the influence of magnetic ordering on the lattice dynamics and electronic structure can be gained by complementing the present results with data from Raman spectroscopy and neutron scattering experiments.

Acknowledgments

The authors wish to thank A Sacchetti for fruitful discussions. This work has been supported by the Swiss National Foundation for Scientific Research within the NCCR MaNEP pool.

References

- [1] Lemmens P, Güntherodt G and Gros C 2003 *Phys. Rep.* **375** 1 and references therein
- [2] Perucchi A, Degiorgi L, Berger H and Millet P 2004 *Eur. Phys. J. B* **38** 65
- [3] Caimi G, Degiorgi L, Kovaleva N N, Lemmens P and Chou F C 2004 *Phys. Rev. B* **69** 125108

- [4] Caimi G, Degiorgi L, Berger H and Forró L 2006 *J. Phys.: Condens. Matter* **18** 4065
- [5] Becker R, Johnsson M, Kremer R K, Klauss H H and Lemmens P 2006 *J. Am. Chem. Soc.* **128** 15469
- [6] Damascelli A, van der Marel D, Grüninger M, Presura C, Palstra T T M, Jegoudez J and Revcolevschi A 1998 *Phys. Rev. Lett.* **81** 918
- [7] Lorenzana J and Sawatzky G A 1995 *Phys. Rev. Lett.* **74** 1867
- [8] Perkins J D, Graybeal J M, Kastner M A, Birgeneau R J, Falck J P and Greven M 1993 *Phys. Rev. Lett.* **71** 1621
- [9] Takahashi Y, Yamasaki Y, Kida N, Kaneko Y, Arima T, Shimano R and Tokura Y 2009 *Phys. Rev. B* **79** 214431
- [10] Wooten F 1972 *Optical Properties of Solids* (New York: Academic)
- [11] Dressel M and Grüner G 2002 *Electrodynamics of Solids* (Cambridge: Cambridge University Press)
- [12] Stokes H T and Hatch D M 1999 SMODES, www.physics.byu.edu/~stokesh/isotropy.html
- [13] Caimi G, Degiorgi L, Berger H and Forró L 2006 *Europhys. Lett.* **75** 496